Chapter 3

Synthesis of Li/TiO_2 catalyst for synthesis of biodiesel derived glycerol to glycerol carbonate

3.1. Introduction

This chapter includes the synthesis of Li modified titanium oxide catalyst as a heterogeneous catalyst by wetness impregnation method and its application in synthesis of glycerol carbonate. In this work, Li was doped on TiO_2 support at different wt.% varies from 10, 20, 30, 40 wt.%. These catalysts were calcined at various temperatures ranging between 350 to 750 ℃ and further tested their catalytic activity towards glycerol conversion. The designed catalyst was studied by performing various characterization techniques such as XRD, TGA-DTA, XPS, FT-IR, FESEM-EDAX, and TEM analysis to obtain its physicochemical properties. ^{1}H and ^{13}C NMR spectroscopic methods were performed to determine the conversion of glycerol-to-glycerol carbonate. Our research approach has been focused towards the synthesis of titania-based heterogeneous catalysts for the valorisation of Gly to GlyC owing to its large surface area, high photo stability, and its acidic-basic nature depending on the active metal loading enhances the catalytic stability and activity under reaction conditions. The incorporation of Li on titania support generates the strongest basic sites than remaining alkali or alkaline metal ions due to its high ion size effect and high molar concentration. Li/TiO_2 has been successively employed in various fields, for instance in electrochemical applications, as a candidate for photo catalyst etc. But reports on its potential application for transesterification reaction have not been studied. In view of above-mentioned physiochemical properties, we synthesized Lithium titanate through the wetness impregnation process and utilize it for green, facile and efficient production of GlyC.

3.2. Synthesis of Li/TiO_2 catalyst

Li/TiO_2, a heterogeneous catalyst was prepared by wetness – impregnation process and subsequent thermal treatment. Initially, solution of pure TiO_2 was dissolved in a requisite amount of double distilled water. LiOH solution was prepared by dissolving the required amount of LiOH in double distilled water as per loading percent. Both the solutions were mixed under constant stirring for 12

hours then the remaining water was evaporated at 120 ℃ under continual stirring till it forms xerogel. The obtained white solid was dried at 110 ℃ for 12 hours, further catalyst was calcinated in a muffle furnace in airflow at a temperature 650 ℃ for 4 hours. The synthesis procedure is depicted below in Figure 3.1.

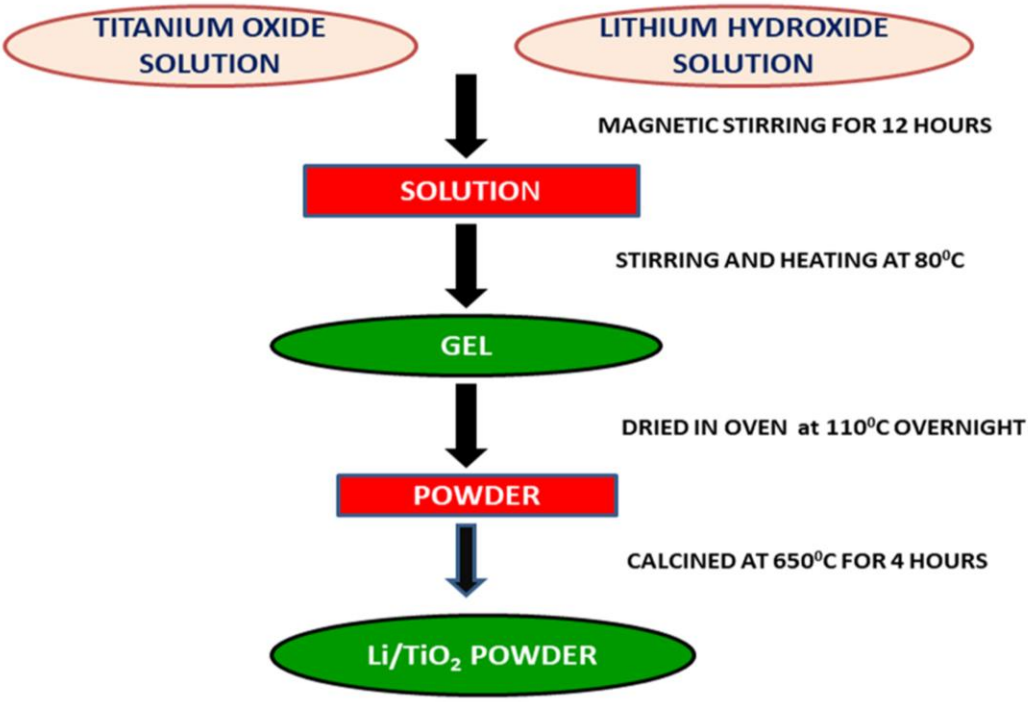

Figure 3.1 Synthesis of Li/TiO_2 catalyst.

3.3. Characterizations of catalyst

3.3.1. XRD studies

The X-ray diffraction peaks of TiO_2 & Li doped TiO_2 with varying loading % calcined at 650 ℃ is shown in Figure 3.2(a), The X-ray diffractogram of Li/TiO_2 with varying lithium concentration (5-35 wt.%) appears at 2θ values 25.15, 36.63, 37.38, 38.31, 47.78, 54.75, 62.19, 69.88, 75.57 with miller indices (101), (004), (200), (105), (211), (204) respectively corresponds to the anatase phase of TiO_2 including some of the minor peaks of rutile appears at 68.36°, 74.95° with miller indices (220), (215) respectively. New diffraction peaks were observed as the lithium content increased.

At lower lithium concentration, mixed-phase of TiO_2, $(Li_2TiO_3)_{10.667}$, Li_2TiO_3 appeared. With increasing lithium concentration gradually to 35 wt.(weight)% on TiO_2, new diffraction peaks were observed at 2θ values 18.35, 43.60, 63.48 with miller indices (111), (400), (440) respectively indicates the formation of $(Li_2TiO_3)_{10.66}$ phase. The diffracted peaks were sharp and intense showing the crystalline nature matched with JCPDS file no. 75-1602 assigned to $(Li_2TiO_3)_{10.667}$ phase having face-centered cubic crystal system, space group – Fd3m [227] & cell parameters a = b = c = 8.2850 A^0, α = β = γ = 90 ^{0}C. In the diffractogram, no diffraction peaks were observed for Li_2O or LiOH which might be due to the higher dispersion of Li ions on the titanium oxide surface [102]. Also, it has been found in studies that Z (atomic number) influences the scattering factor; accordingly, the lighter atoms are weakly diffracted and undetected in the presence of heavier atoms like titanium metal [103]. Therefore, Li peaks were absent in the diffractogram due to the high scattering factor of Ti as compared to Li atom. In Figure 3.2(b), the impact of calcination temperature on the crystal structure has also been studied, and it was found that at 450-650 ℃, low crystalline peaks at 36.25, 40.01, 48.93, 75.22 attributes to Li_2TiO_3 and peaks at 37.03, 63.48 corresponds to $LiTiO_2$. Further, with increasing temperature to 650 ℃, the intense sharp peak appears at 18.35, 30.62, 36.25, 43.60, 57.07, 63.48; as the $LiTiO_2$ phase converted into $(Li_2TiO_3)_{10.66}$ as a result of the solid-state reaction between precursors LiOH & TiO_2 indicates the formation of $(Li_2TiO_3)_{10.66}$ phase. With increasing temperature to 750 ℃, some extra peaks of Li_2TiO_3 were observed. This ascribed to the modification in the crystal structure with lowering crystallinity due to interaction between metals [104].

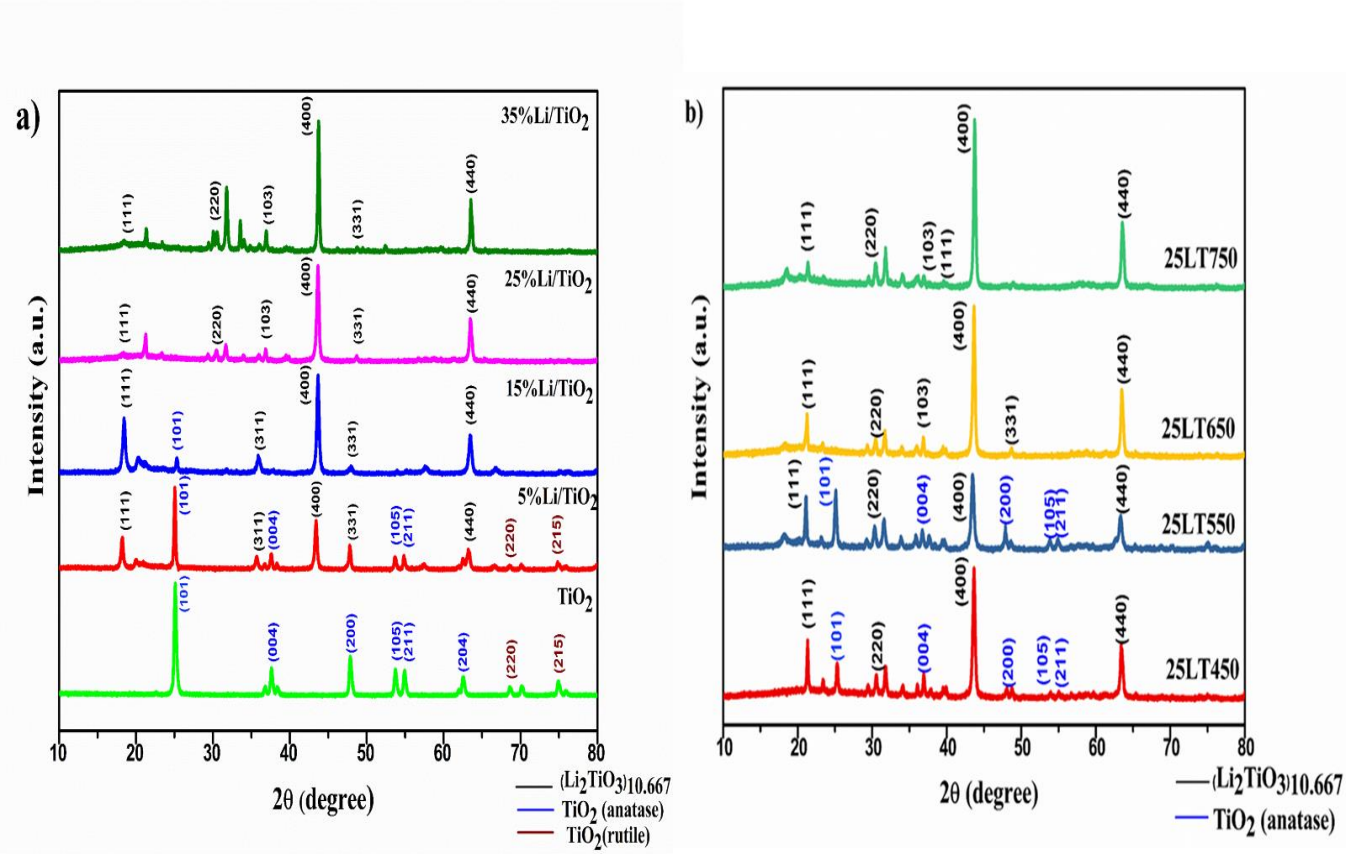

Figure 3.2 XRD patterns of (a) Pure TiO_2 and TiO_2 with different loading wt.% of LiOH (b) 25 wt.% LiOH loaded on TiO_2 calcined at different calcination temperatures.

3.3.2 Thermogravimetric analysis of Li/TiO_2

The thermo gravimetric analysis of Li/TiO_2 catalyst is presented in Figure 3.3. The heating process of synthesized catalyst involves the first stage of weight loss around 100 ℃ owing to the loss of adsorbed water on the crystal lattice corresponds to the endothermic peak around the same temperature. The second stage of weight loss was observed around 600 ℃, the DTA curve supports the endothermic heat flow around 600 ℃ due to thermal breaking of bond and formation of bond between Li and Ti metals. No weight loss was observed between 200 ℃ and 400 ℃ but an endothermic heat flow observed between 200 ℃ and 400 ℃ due to interference between Li and

TiO_2. Further, no weight loss occurred after 600 °C attributes to the thermal stability of the compound. Therefore, the calcination temperature 650 °C was chosen as the stable temperature for 25 wt.% Li/TiO_2.

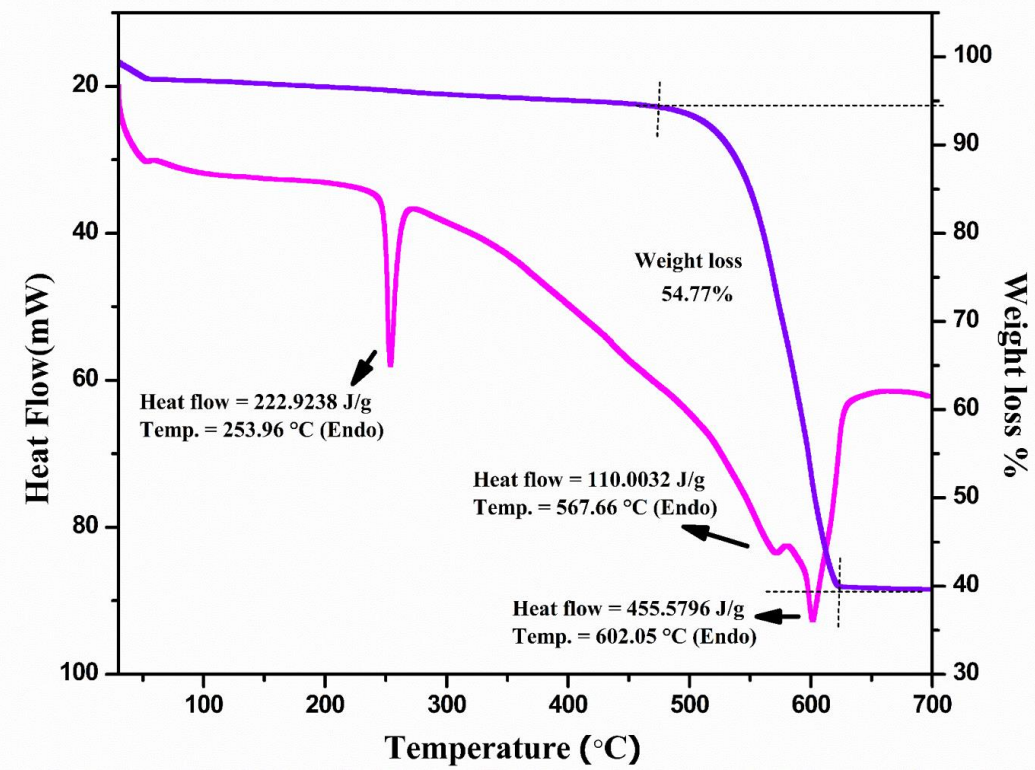

Figure 3.3. TGA – DTA plot of 25 wt.% Li/TiO_2 (without calcination).

3.3.3 XPS studies of the synthesized catalyst

The surface chemical analysis of 25 wt.% Li/TiO_2 catalyst was explored using XPS and the graphs are depicted in Figure 3.4. The XPS peaks of different elements were calibrated, taking the C1s peak (284.8 eV) as the reference. The XPS survey peak evident the presence of Li, Ti, O in the synthesized catalyst. The small peaks that appear between 0-100 eV confirm the existence of Li metal, which cannot be identified using EDS spectra. In the Ti spectrum, Ti 2p appears at binding energies 458.39 eV, 464 eV corresponds to Ti $2p_{3/2}$ and Ti $2p_{1/2}$ with a doublet splitting of 5.7 eV due to spin-orbit coupling of Ti 2p correspond to Ti^{+4} [105]. In the O1s XPS spectrum, peaks

appear at binding energy 529.90 eV due to Li-O and Ti-O bonding. Further, the peak at 531.87 eV is due to Li_2CO_3 formation due to the adsorption of ambient CO_2 in the metal lattice. In Li spectra, two peaks were depicted; peak at 55.23 corresponds to the characteristic peak of Li_2O, which shows a shift from 55.6 eV to 55.23 eV due to the impregnation of Li metal indicates the change in the chemical environment of crystal. Additionally, the peak at 62 eV indicates the presence of Ti 3s [106]. The results are in accordance with the Thermo Fisher XPS database and the oxidation states of the elements present shows validation with the XRD results.

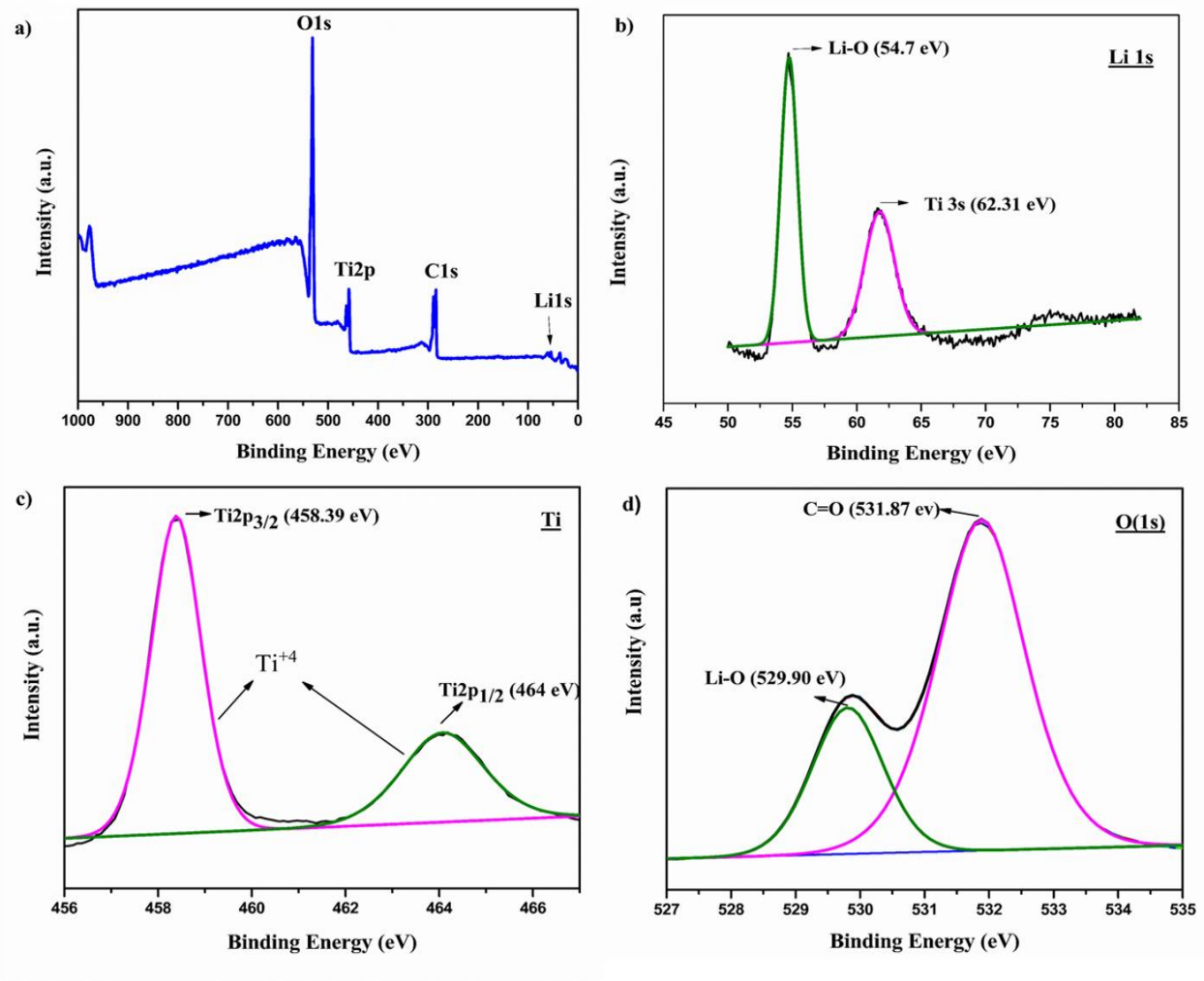

Figure 3.4. XPS plots of (a) survey peak of sythesized 25 wt.% Li/TiO_2, (b) Li (1s) spectra, (c) Ti spectra, (d) O (1s) spectra.

3.3.4 Basicity of Li/TiO_2

The total basicity of the surface-active sites of the synthesized catalyst was examined by using Hammett indicator analysis. Benzene solution containing different adsorbed catalysts i.e., TiO_2, 5 wt.% Li/TiO_2 650 ℃, 25 wt.% Li/TiO_2 650 ℃, 25 wt.% Li/TiO_2 750 ℃ undergoes titration with benzoic acid. It was noted that with increasing the lithium concentration from 5 wt.% to 25 wt.%, the basic strength comes in the range $15 < H_- < 18.4$ illustrated in Table 3.1. The basic amount of the synthesized 25 wt.% Li/TiO_2 is 19.54 mmol/g. Further, increasing concentration increases the basic strength to above $18.4 < H_- < 27$, which leads to the decarboxylation of the GlyC results in glycidol formation [52][107][108].

Table 3.1. Basic amount and surface properties of the as synthesized catalyst.

Catalyst	Basic strength	Basic amount (mmol/g)	Average particle size (nm)
TiO_2	$H_- < 15$	3.8	54.3
5 wt.% Li/TiO_2 650 ℃	$15 < H_- < 18.4$	13.9	52.2
25 wt.% Li/TiO_2 650 ℃	$15 < H_- < 18.4$	19.5	49.4
25 wt.% Li/TiO_2 750 ℃	$18.4 < H_- < 27$	22.3	126.4

3.3.5. FT-IR analysis of Li/TiO_2

The functional groups present on the surface of synthesized catalyst (Li/TiO_2) were investigated by FT-IR analysis illustrated in Figure 3.5. The characteristic IR absorption bands ranging between 400-4000 cm^{-1} were studied. The intense vibration band in the range 400 – 850 cm^{-1} represents the metal-oxygen bond vibrations. It is clear from the graph that with increasing lithium concentration,

the broad band of TiO_2 becomes sharper and the peak at 862 cm^{-1} represents the formation of mixed metal oxide [109]. The intense split absorption bands at 1435, 1505 cm^{-1} belongs to C=O bond vibration of CO_3^{2-} due to the CO_2 adsorption on the crystal lattice. Further, the band at 1635 cm^{-1} represents the O-H bending vibration, which disappears with increasing loading %. The broad spectrum at 3400 cm^{-1} is because of the stretching vibration of surface water molecules [55]. The FTIR analysis is analogous with XRD data showing Li is impregnated successfully on TiO_2 lattice.

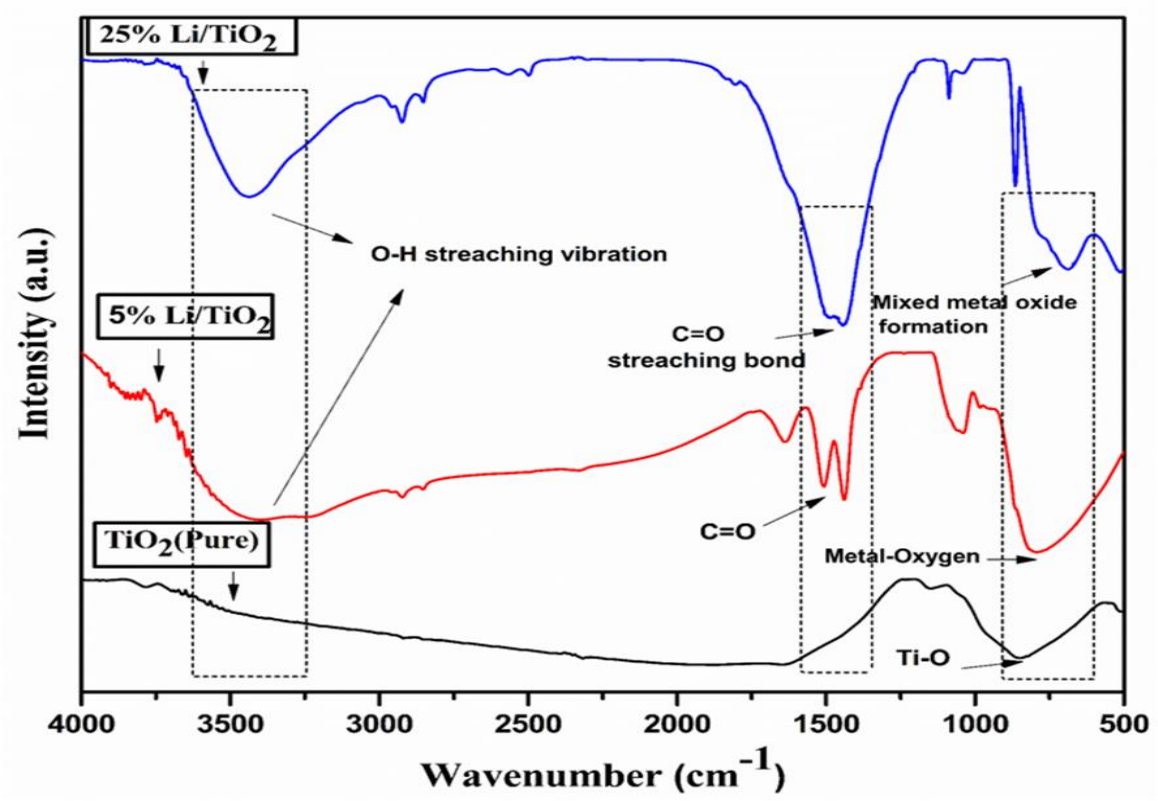

Figure 3.5. FT-IR spectra of TiO_2 Pure, 5 wt.% Li/TiO_2, 25 wt.% Li/TiO_2.

3.3.6. FE-SEM studies of Li/TiO_2

The surface morphology and elemental analysis of the synthesized catalysts were explored by FESEM-EDAX images (Figure 3.6). Figure 3.6A shows the FE-SEM image of pure TiO_2 illustrates that the particles are spherical and relatively porous in morphology with the average

particle size 54.34 nm. In Figure 3.6B, the FE-SEM image shows the crystal starts growing with increasing Li loading on TiO_2 and the average particle size of grains of 5 wt.% Li/TiO_2 is 52.19 nm. Further, with increasing Li concentration to 25 wt.% of TiO_2, leads to formation of $(Li_2TiO_3)_{10.66}$ crystal with the average particle size 49.39 nm indicates that the synthesized catalyst is a nano catalyst (Figure 3.6C). Moreover, calcination temperature also has profound effect on the size of the particle, and at 750 ℃, agglomeration starts, and the average particle size comes to be 138.18 nm illustrated in Table 3.2 (Figure 3.6D). Particle size increases, suggesting the growth of the catalyst with increasing Li loading. It was studied earlier that at higher temperature solid-phase reaction results in the deformation of the metal oxide crystals leads to the particle growth and sintering of the catalyst [110, 111]. The analysis shows that the catalyst is porous, and particles have irregular spheroid morphology with varying grain sizes. The result is analogous to XRD results shows the formation of a new phase with increasing temperature. The morphology of the recycled catalyst remains the same, confirming that catalyst is stable during reaction. The EDAX study validate the existence of Ti and O elements; Li was not detected due to the atomic mass detection limit of the instrument (Figure 3.6E).

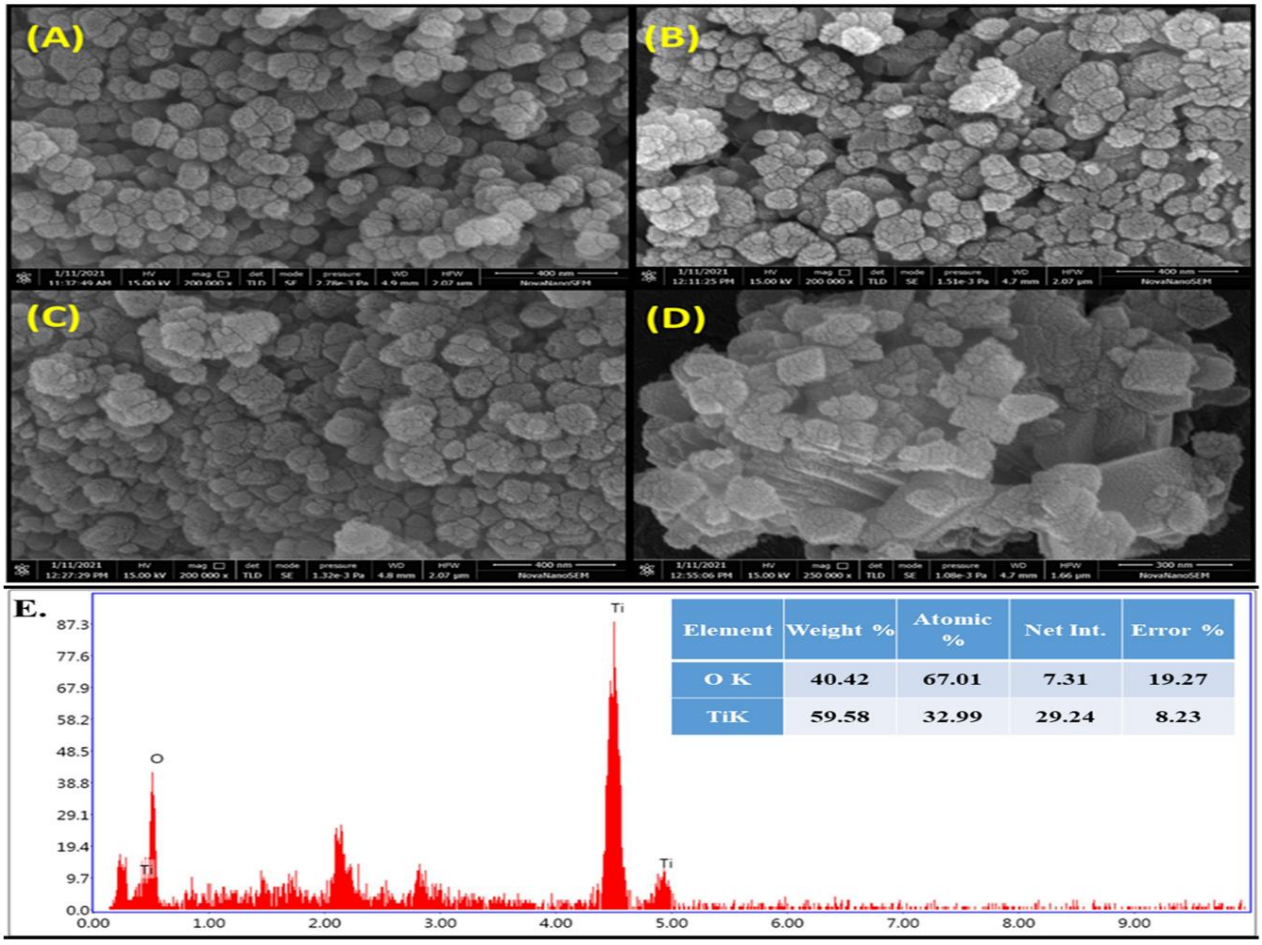

Figure 3.6. FE-SEM images of (A) Pure TiO_2, (B) 25 wt.% Li/TiO_2 calcined at 650 ℃ , (C) Recycled 25 wt.% Li/TiO_2 calcined at 650 ℃ (D) 25 wt.% Li/TiO_2 calcined at 750℃ and (E) EDAX spectra of the synthesized 25 wt.% Li/TiO_2.

3.3.7 TEM studies of Li/TiO_2

The TEM image of the synthesized catalyst is depicted in Figure 3.7. The phases can be clearly seen in the micrographs. In Figure 3.7A, it is evident from the image that the crystallites of 25 wt.% Li/TiO_2 fused together to form an agglomerate of particles of wide-ranging sizes having deformed spherical shape. In Figure 3.7B, the appearance of two types of particles showing adsorption of one particle above the other confirms the impregnation of Li on TiO_2 [112]. In Figure 3.7C, the HR micrograph with well-resolved lattice fringes is observed, the lattice fringes are

aligned in a parallel manner, the d- spacing values of the inter planer fringes comes to be 0.29 nm, which corresponds to the (220) plane of $(Li_2TiO_3)_{10.667}$ matched with JCPDS file no. 75–1602. In Figure 3.7D, the histogram represents the average particle size of different crystallites which comes to be 65.26 nm. The results are in accordance with XRD studies.

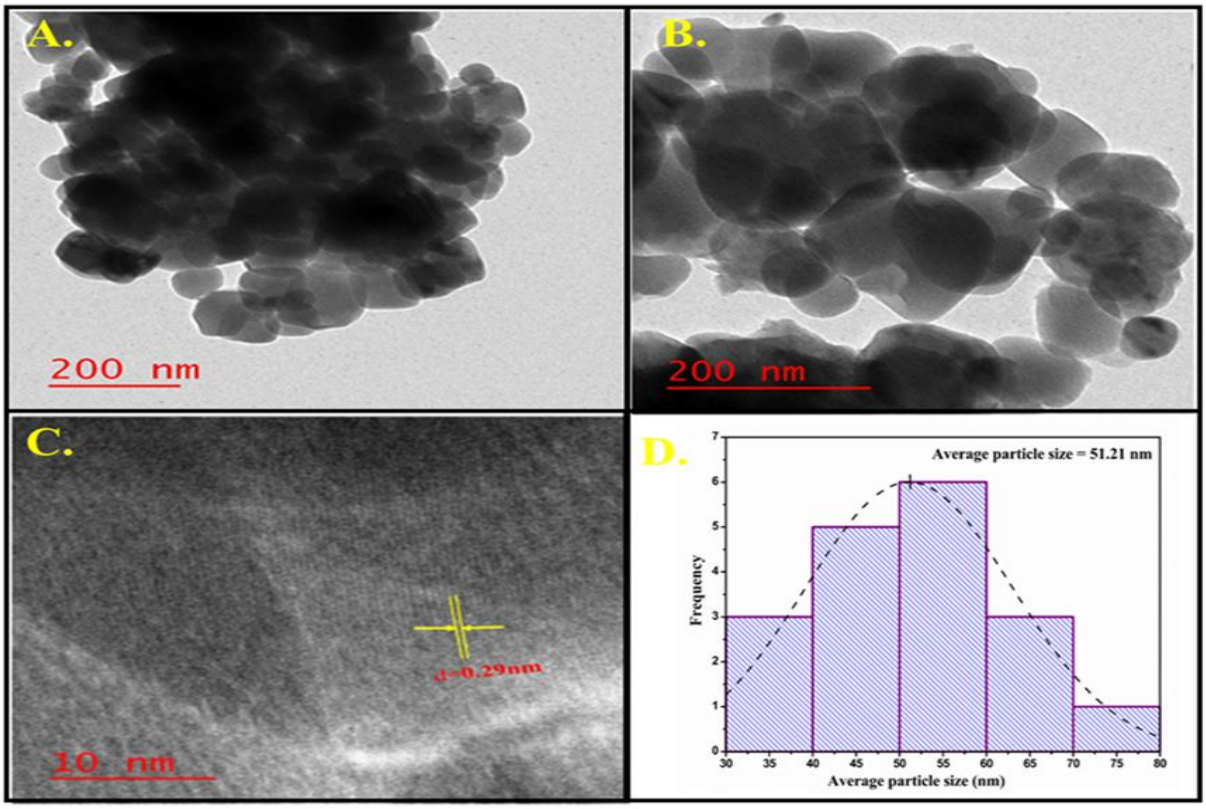

Figure 3.7. TEM images of synthesized 25 wt.% Li/TiO_2

3.4 Evaluation of activity of catalyst for glycerol carbonate synthesis

3.4.1 Selection of active catalyst

On the basis of basic strength, a series of alkali metals loaded on titania-based catalysts were synthesized. The catalytic activity was investigated for the transesterification of Gly with DMC to yield glycerol carbonate (Scheme 3.1). Studies have found that alkali metal oxides enhance the basic nature of the catalysts. Clearly, among the various metal-loaded catalysts, Li/TiO_2 shows the

best results with glycerol conversion of 95.51% and 95.88 % glycerol carbonate selectivity. Li/γ-Al_2O_3, Li/ZrO_2 shows lower conversion with lesser selectivity towards glycerol carbonate formation ascribed in Table 3.2. Therefore, Li/TiO_2 selected as the best catalyst for glycerol carbonate conversion.

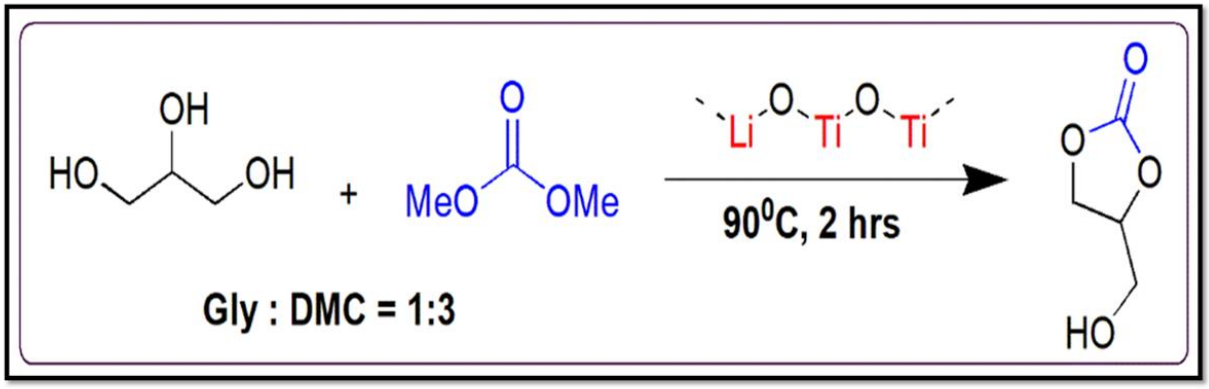

Scheme 3.1. Transesterification reaction of Gly with DMC.

Table 3.2. Screening of catalyst and effect of calcination temperature for synthesis of glycerol carbonate

Catalyst	Conversion (%)	Selectivity (%)		Yield (%)
		GlyC	GD	
TiO_2	3.5	94.5	5.5	3.3
LiOH	20.8	94.3	5.7	19.6
25 wt.% Li/TiO_2 650 ℃	95.5	95.9	4.1	91.6
25 wt.% Li/TiO_2 450 ℃	35.6	91.7	8.3	32.7
25 wt.% Li/TiO_2 550 ℃	52.4	92.6	7.4	48.5
25 wt.% Li/TiO_2 750 ℃	86.0	94.7	5.3	81.4
Li/γ-Al_2O_3 650 ℃	80.4	95.3	4.7	76.6
Li/ZrO_2 650 ℃	78.3	95.5	4.5	74.8

Reaction conditions – Gly:DMC = 100 mmol:200 mmol, catalyst dose – 0.46 gm, reaction temperature – 90 ℃, time – 2 hours
where, Yield (%) = % of conversion of glycerol × % of selectivity of GlyC; GlyC – glycerol carbonate, GD – glycidol

3.4.2 Calcination temperature

Studies have found that calcination temperature changes the composition of the mixed metal oxides along with their acidic and basic properties. The synthesized catalyst showed the best activity at 650 ℃ with the formation of the crystal phase. Furthermore, the dependence of calcination temperature on the catalytic activity was explored. The 25 wt.% Li/TiO_2 was calcined at 450 ℃, 550 ℃, 650 ℃, 750 ℃ and employed for the conversion of Gly to GlyC. Lower conversion was obtained when the synthesized catalyst was calcinated at 450 ℃. The catalytic activity increases rapidly as the calcination temperature raised to 650 ℃ and decreases after a further rise in calcination temperature. Pre-treated catalyst at 650 ℃ shows the best catalytic activity and gives the highest conversion of 95.51% and selectivity to 95.88 %. Increasing the calcination temperature decreases the selectivity towards GlyC because of the generation of stronger basic sites that leads to the decarboxylation of the GlyC to form glycidol. Also, the elevated temperature may lead to the sintering of the catalyst resulting in loss of activity of the catalyst illustrated by FE-SEM analysis.

3.4.3 Effect of loading percentage

The glycerol conversion was checked with varying loading percentage of the lithium metal over titania from 5 to 35 wt.%, and it was found that with increasing lithium concentration, glycerol conversion increases to 95.51 % and selectivity to 95.88 %. Further, with growing lithium concentration, the conversion would not increase also, but selectivity starts decreasing due to decarboxylation of GlyC arises owing to the high basicity of the catalyst [113].

3.4.4 Characterization of synthesized product

3.4.4.1 ^{1}H and ^{13}C NMR of the synthesized glycerol carbonate

After completion of the reaction, the catalyst present in the reaction matrix was filtered out through Whatman filter paper, and the filtered reaction mixture undergoes rotatory evaporation of the unreacted DMC and methanol as the unreacted DMC and methanol present in the reaction matrix forms the lower boiling azeotropic mixture. further, the synthesized compound undergoes NMR analysis using NMR spectrometer. Deuterated dimethyl sulfoxide was used as the solvent. The ^{1}H and ^{13}C NMR spectra of the synthesized compound is shown in Figure 3.8(a) and Figure 3.8(b), and it is observed that the multiplet peak at 4.81 ppm is primarily accountable for determining the conversion percentage of glycerol carbonate formed. The conversion % can be calculated by the integration peak area of ^{1}H NMR of methine proton of glycerol carbonate at chemical shift 4.81 ppm and integration peak area of methine proton of Glycerol at chemical shift 3.43 ppm (Figure 3.8(a)) [115, 116].

The formula is depicted below –

$$\textbf{Conversion \% = \% } C_{Gly} = \frac{Ia1}{Ib+Ia2} \times 100 \qquad (3.1)$$

where, I_{a1} = Integration of one of the methylene protons of glycerol carbonate (3.736 – 3.793 ppm), and $I_b + I_{a2}$ = Sum of the integration of methine proton of glycerol (b) and integration of methylene proton of glycerol carbonate(a_2) (3.557 – 3.640 ppm). Figure 3.8b depicts the ^{13}C spectra of glycerol carbonate. The appearance of characteristic chemical shift peaks at 61.06, 66.33, 77.49, 155.65 ppm validate the formation of glycerol carbonate. Peak around 40.45 ppm shows the DMSO-d_6 solvent peak. Peaks at 66.33, 77.49, 61.06 ppm represent C_2, C_3, C_4 carbon of glycerol carbonate moiety, and peak at 155.65 represents the carbonyl group of the dioxolane ring.

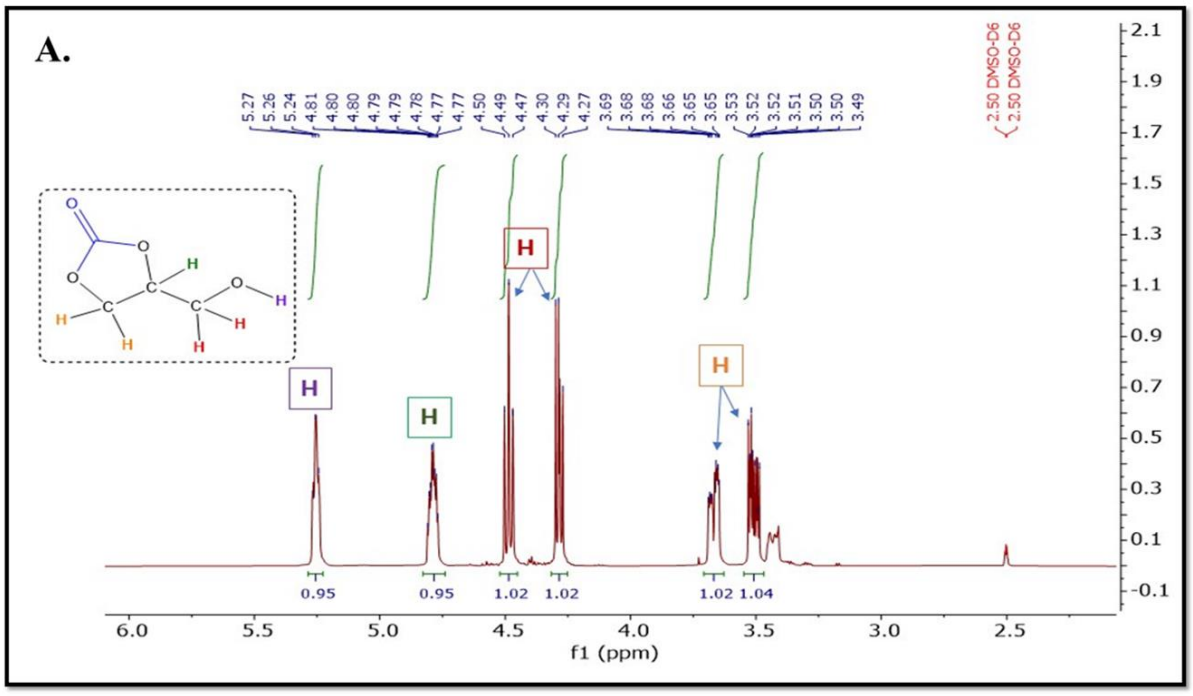

Figure 3.8. (a) ^{1}H-NMR spectra of the synthesized glycerol carbonate

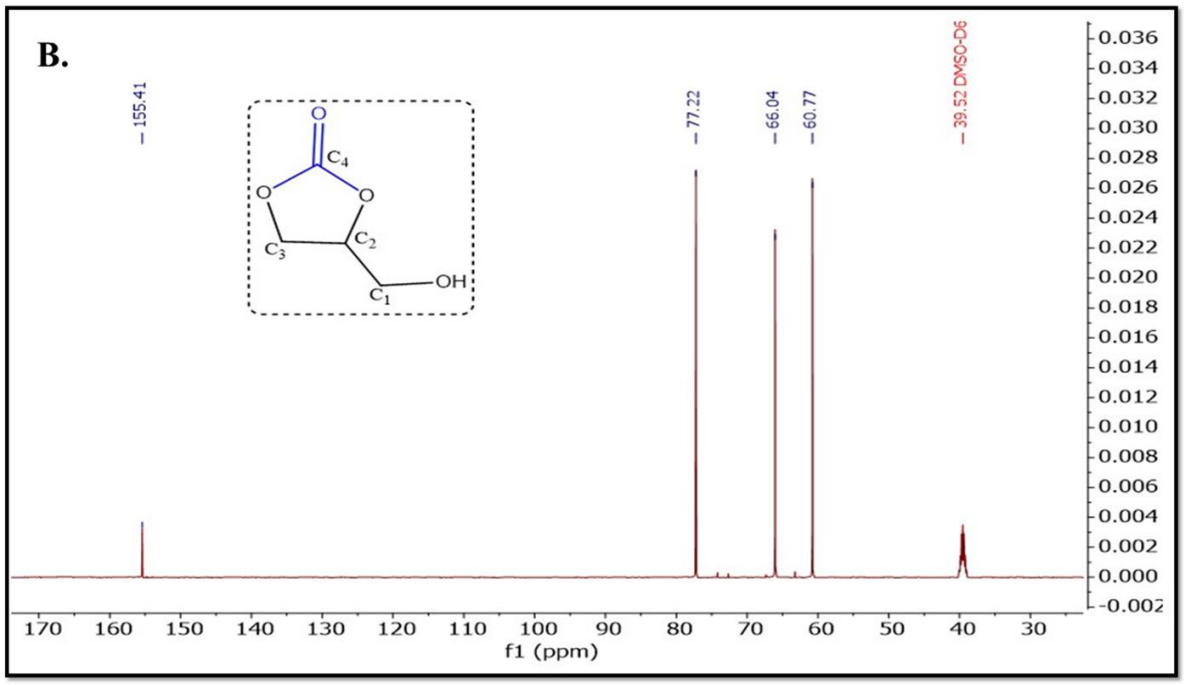

Figure 3.8 (b) ^{13}C-NMR of the synthesized glycerol carbonate.

3.4.5 Proposed reaction mechanism

The Li/TiO_2-catalyzed transesterification of Gly with DMC to produce GlyC proceed through various steps, as illustrated in Scheme 3.2. It is proposed to follow the Langmuir−Hinshelwood mechanism (L-H), and it proceeds similarly as reported previously with other mixed metal oxide catalysts [117, 118, 119]. Glycerol interacts with the basic sites (Li); meanwhile, DMC interacts with acidic sites (Ti) available on the surface of the catalyst, and both come in close proximity (A). The basic sites(Li) of the catalyst deprotonate the primary -OH group of Gly (B) [120]. The Lewis acidic sites (Ti) of the prepared catalyst coordinates with the carbonyl group of DMC and enhances its electrophilicity [121]. The activated carbonyl group of DMC then undergoes a nucleophilic attack by deprotonated primary -OH group of Gly that results in the removal of one methanol molecule to afford an intermediate (C) [122]. The formed intermediate (C) undergoes nucleophilic substitution (intramolecular) to afford the desired product GlyC. During the process, another methanol molecule is eliminated.

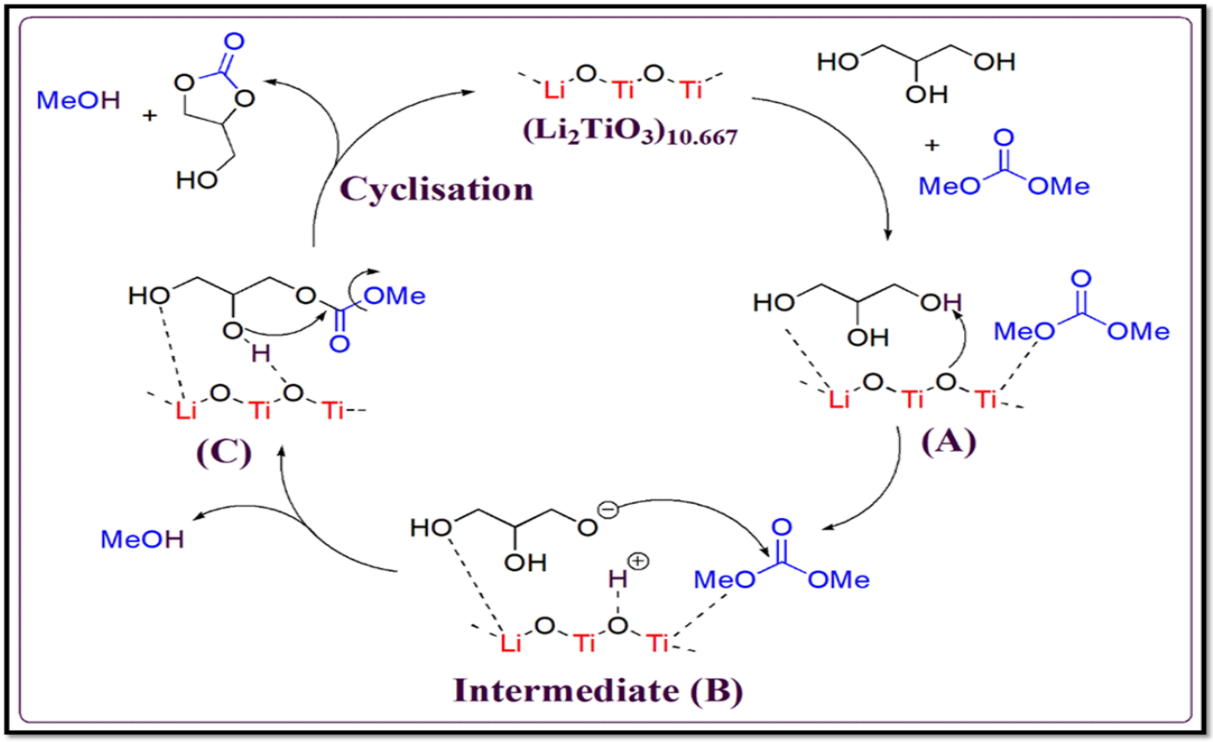

Scheme 3.2. Proposed reaction mechanism for the role of 25 wt.% Li/TiO_2 for the transesterification of glycerol with DMC.

3.5. Optimization of reaction parameters

3.5.1 Influence of molar ratio on conversion

The transesterification reaction of Gly with DMC is reversible. In order to shift the equilibrium, forward a higher stoichiometric ratio of DMC to Gly is required. In this study, at 1:1 stoichiometric ratio of Gly to DMC, the conversion of Gly to GlyC is found to be 43.6%, at 1:2 Glycerol to DMC molar ratio, conversion obtained was 75.22%, which increases to 95.51% at 1:3 which further decreases with increasing Gly to DMC molar ratio. Since the hydrophobic and hydrophilic nature of DMC and Glycerol respectively makes the reaction matrix a biphasic system. Excess DMC restricts the biphasic system and promotes the reaction between Glycerol and DMC. Thus, the optimum molar ratio of Glycerol to DMC achieved to be 1:3 which gives highest conversion towards glycerol carbonate (Figure 3.9A) [123, 124].

3.5.2 Influence of reaction temperature

During transesterification reaction, an increase in temperature would cause the reactant molecules to collide faster, resulting in higher product formation. Therefore, to determine the optimum temperature which higher glycerol carbonate yield is achieved, transesterification at a different temperature from 65 ℃ to 95℃ was investigated. It was found that the highest conversion is obtained at 90 ℃. Further increasing the temperature would decrease the product yield (Figure 3.9B) [108, 125].

3.5.3 Influence of catalyst dose

To examine the optimum amount of catalyst required for attaining the maximum Gly conversion to yield GlyC, catalyst concentration in the reaction matrix was varied from 1 to 7 weight % and conversion was checked, and it was found that the glycerol conversion increases with increasing catalyst dose as a higher concentration of catalyst contains a greater number of active surface sites which facile the substrate molecule to react leads to higher glycerol

conversion and yield. However, no significant increase in conversion was observed with further increase in catalyst dose because higher dose of catalyst enhances the viscosity in the reaction matrix, which hinders the interaction between reactants and the catalyst. Consequently, the optimum dose of catalyst for the transesterification is selected to be 5 wt.% (Figure 3.9C) [66, 121, 122, 126].

3.5.4 Influence of reaction time

The reaction time for the conversion of glycerol-to-glycerol carbonate was also optimized, and it was found to achieve the maximum transformation (95.51%) within the span of 2 hours. As the reaction time increases, the conversion % starts decreasing because of reaching the equilibrium in the transesterification reaction within this time span. Further decarboxylation of glycerol carbonate leads to reduced conversion % [122, 127]. Therefore, the reaction time optimization has its own influence in attaining the best conversion because the generation of glycidol predominates over the GlyC after the optimized time period (Figure 3.9D).

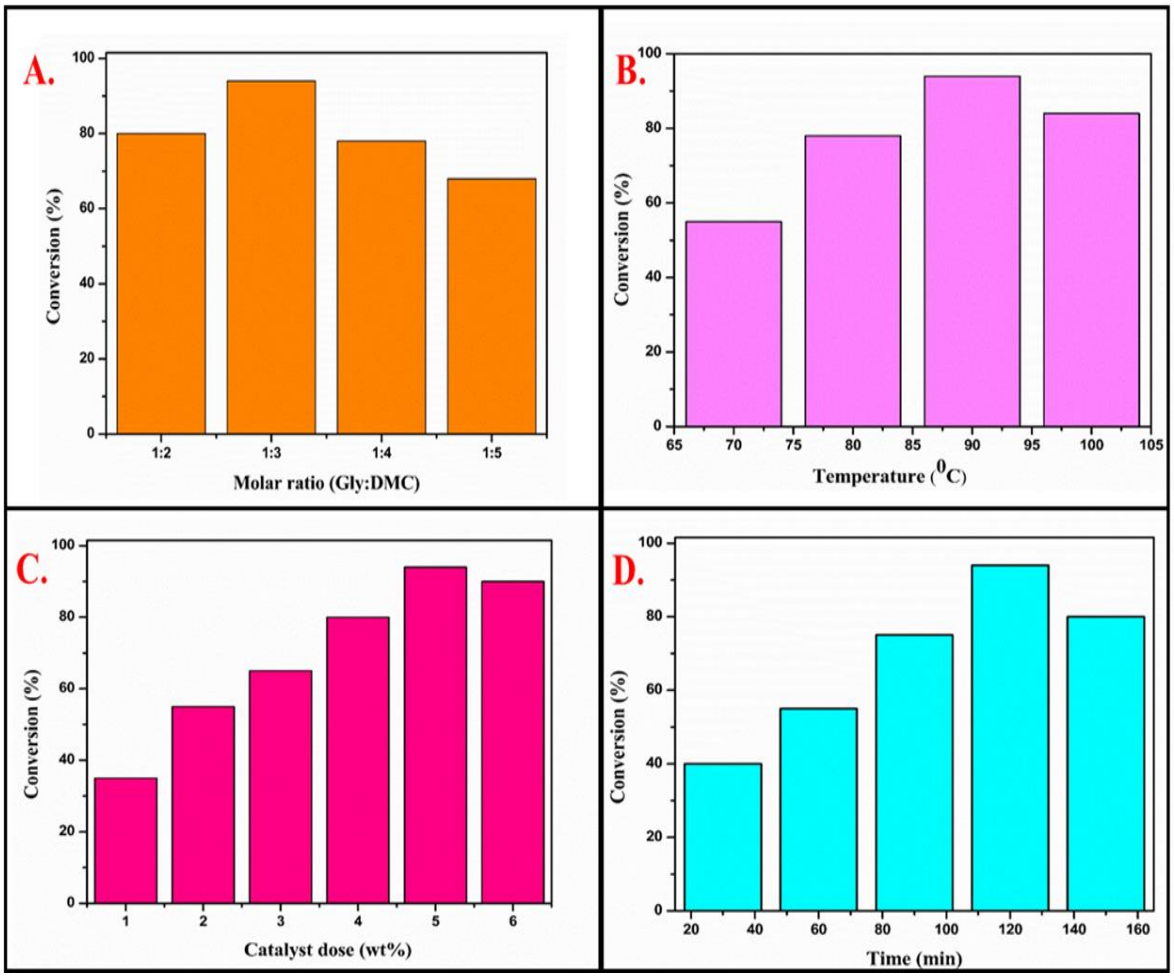

Figure 3.9. Effect of reaction parameters (A) Molar ratio (reaction conditions: catalyst dose = 5 wt.% with respect to glycerol used, reaction temperature = 90^{0}C, reaction time = 2 hrs), (B) Temperature (GLY:DMC = 1:3, catalyst dose = 5 wt.%, reaction time = 2 hrs) (C) Catalyst dose (reaction temperature = 90^{0}C, reaction time = 2 hrs, GLY:DMC = 1:3) (D) Reaction time (GLY:DMC = 1:3, catalyst dose = 5 wt.% reaction temperature = 90^{0}C).

3.6. Recyclability of the catalyst

The reusability test of the catalyst is performed and it was found that 25 wt.% Li/TiO_2 is reusable under optimized reaction condition. Before reuse, the catalyst was recovered from the mixture through centrifugation, washed with methanol and dried at 110 ℃ followed by recalcination at 650 ℃. The catalytic activity of regenerated catalyst without recalcination has lesser conversion than that of recalcined one because of the change in the active phase of the catalyst as depicted by XRD data (Figure 3.10 (a)). The recovered catalyst can be used for up

to 5 reaction cycles. The conversion and yield of glycerol carbonate slightly decrease upon successive runs because of the leaching of lithium in the reaction matrix and loss of active sites due to pore filling by reactant molecules. The recyclability shows the stability of the catalyst (Figure 3.10 (b)). In order to determine the loss of active site due to leaching of the catalyst, ICPMS analysis were performed of fresh and reused catalyst (after 5 cycles). ICP-MS analysis reveals that the concentration of Lithium metal in the 25 wt.% Li/TiO_2 in the present in the active site of the catalyst decreases. The concentration of the Li metal decreases from 1.878 ppm (fresh catalyst) to 1.282 ppm by the end of 5^{th} reaction cycle obtained by ICPMS analysis (Figure 3.10 (c)). This indicated that the catalytic activity towards transesterification reaction of glycerol-to-glycerol carbonate is reduced due to the leaching of the Li metal during reuse.

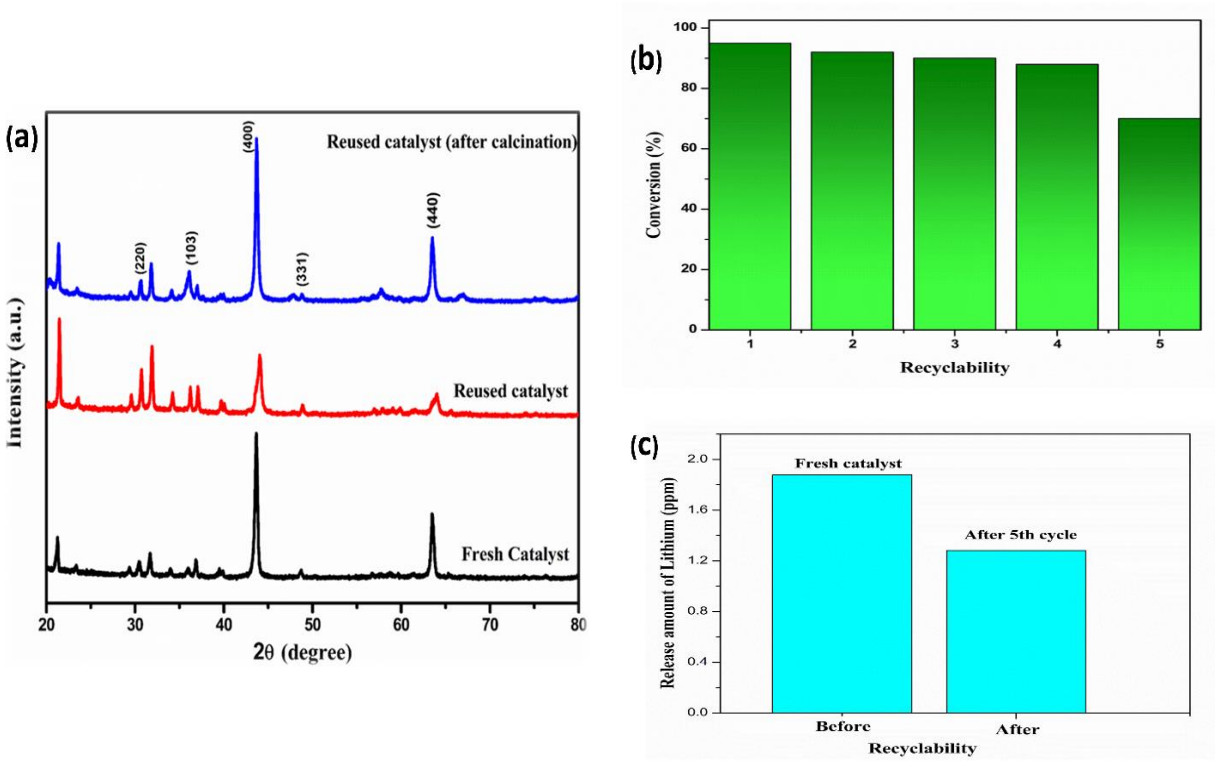

Figure. 3.10 . (a) XRD diagram of fresh catalyst, reused catalyst (without calcination), and reused catalyst (after calcination), (b) Reusuability of as prepared 25 wt.% Li/TiO_2, (c) ICPMS Analysis of fresh 25 wt.% Li/TiO_2 catalyst and reused 25 wt.% Li/TiO_2.

3.7. Comparative study of synthesized 25wt% Li/TiO_2 with previously reported catalyst

The catalytic stability, reusability, catalytic activity of the synthesized 25 wt.% Li/TiO_2 towards transesterification reaction of glycerol with DMC is compared with the previously reported catalysts presented in Table 3.3. The earlier reported Ti based catalyst i.e. Ti-SBA-15 [118] showed a substantial activity but gives low yield of GlyC. Also, the catalyst undergoes recyclability up to 4th reaction cycle with the conversion of only 63 %. In contract to this, the synthesized catalyst 25 wt.% Li/TiO_2 catalyst showed good activity and conversion of 95.51 % and yield of 91.58 % towards glycerol carbonate production. Also, the catalyst showed better reusability up to 6 reaction cycles. In a similar way, the other reported catalysts i.e. Mg/Zr/Sr [122], KF/La-Zr [121], HTC-Ni [128] show relatively lesser catalytic activity in prospects of reaction duration, DMC: Gly molar ratio, reusability and the solvent used. The relative comparison suggests that the synthesized catalyst showed good catalytic activity towards glycerol carbonate production in comparison to other catalysts.

Table 3.3. Comparison of synthesized 25 wt.% Li/TiO_2 catalyst with previous reports.

Catalyst	**Molar ratio (Gly:DMC)**	**Reaction time (min)**	**Conversion (%)**	**Reusability (Reaction cycle)**	**References**
Ti-SBA-15	1:5	240	94	3rd	[118]
Mg/Zr/Sr	1:5	90	96	4th	[122]
HTC-Ni	1:3	120	55	4th	[129]
KF/La-Zr	1:4	80	91.8	5th	[121]
Li/$Mg_4AlO_{5.5}$	1:3	80	100	Not reported	[107]
25 wt.% Li/TiO_2	1:3	120	95.5	5th	Present study

3.8. Conclusion

The transesterification of bio-waste glycerol with DMC using Li/TiO_2 is proved to be an efficient catalyst with remarkable selectivity and stability. The basic nature of designed catalyst has the major role in excellent yield of GlyC and high conversion percentage of glycerol. The investigation displayed that the activities of pure LiOH and TiO_2 were lower as compared to that of bimetallic mixed oxide since TiO_2 provides very good support in transesterification of glycerol. Characterization of the catalyst by techniques like XRD, FE-SEM, TGA-DTA, XPS etc. proved the presence of combined mixed oxide at preferred loading percentage. The yield of glycerol carbonate depends upon the metallic content and the reaction conditions also. Overall, the catalyst was synthesized from inexpensive materials and it is highly selective, efficient, and recyclable, as a result the catalyst can be best to be fit in production of glycerol carbonate in industrial scale.